Resonance Electron Attachment to Tetracyanoquinodimethane

ARTICLE *in* THE JOURNAL OF PHYSICAL CHEMISTRY A · AUGUST 2014

Impact Factor: 2.69 · DOI: 10.1021/jp505841c · Source: PubMed

4 AUTHORS, INCLUDING:

Stanislav A Pshenichnyuk
Institute of Physics of Molecules and Crystals
58 PUBLICATIONS **293** CITATIONS

THE JOURNAL OF PHYSICAL CHEMISTRY A

Article

pubs.acs.org/JPCA

Resonance Electron Attachment to Tetracyanoquinodimethane

Stanislav A. Pshenichnyuk,*[,†,‡] Alberto Modelli,[§,∥] Eleonora F. Lazneva,[‡] and Alexei S. Komolov[‡]

[†]Institute of Molecule and Crystal Physics, Ufa Research Centre, Russian Academy of Sciences, Prospekt Oktyabrya 151, 450075 Ufa, Russia

[‡]Physics Faculty, St. Petersburg State University, Uljanovskaja 1, 198504 St. Petersburg, Russia

[§]Dipartimento di Chimica "G. Ciamician", Università di Bologna, via Selmi 2, 40126 Bologna, Italy

[∥]Centro Interdipartimentale di Ricerca in Scienze Ambientali, Università di Bologna, via S. Alberto 163, 48123 Ravenna, Italy

ABSTRACT: Resonance interaction of low energy (0−14 eV) electrons with gas-phase 7,7,8,8-tetracyanoquinodimethane (**TCNQ**) was investigated using dissociative electron attachment (DEA) spectroscopy. Spectral features associated with formation of long-lived **TCNQ** molecular negative ions are detected at incident electron energies of 0.3, 1.3, and 3.0 eV. A variety of negative fragments is observed around 4 eV, and slow (microseconds) dissociative decay channels are detected at about 3 eV, in competition with simple re-emission of the captured electron. The average electron detachment time from the $TCNQ^-$ negative ions formed at 3 eV was evaluated to be 250 μs. The experimental findings are interpreted with the support of density functional theory (DFT) calculations of the empty orbital energies, scaled with an empirical equation, and by comparison with earlier electron transmission spectroscopy (ETS) data. A possible mechanism for the unusual formation of long-lived molecular anions above zero energy (up to 3 eV) is briefly discussed. The present results on the interactions between electrons and isolated **TCNQ** molecules could give more insight into processes observed in **TCNQ** adsorbates under conditions of excess negative charge. In particular, electron-stimulated surface reactions are hypothesized, likely occurring when condensed **TCNQ** molecules are exposed to electron beam irradiation.

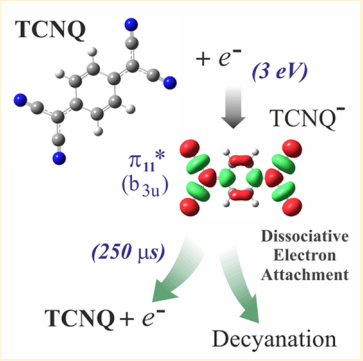

1. INTRODUCTION

Organic molecules with π-conjugated systems are becoming ever more widely used as active elements in novel electronic devices such as organic light-emitting diodes (OLEDs), organic field-effect transistors (OFETs), and organic photovoltaic cells (OPVs).[1−3] Organic crystals formed from the electron acceptor 7,7,8,8-tetracyanoquinodimethane (**TCNQ**, structural formula shown in Chart 1) and the electron donor tetrathiafulvalene

Chart 1. Structure of TCNQ

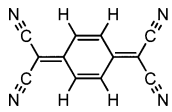

(**TTF**) were discovered in the early 1970s[4] and found to reveal very high, metallic-like electrical conductivity over a wide temperature interval, making them a promising material for organic electronic devices.[5,6] **TTF-TCNQ** systems form a quasi-one-dimensional structure, an organic charge-transfer (CT) salt, where electrons from the highest occupied molecular orbital (HOMO) of the **TTF** molecules are transferred into the lowest unoccupied molecular orbital (LUMO) of the **TCNQ** molecules, leading to stable CT states where the **TCNQ** molecules bear an excess negative charge.

Self-organization of **TCNQ** and its fluorinated analog, 2,3,5,6,-tetrafluoro-7,7,8,8-tetracyanoquinodimethane (**F_4-TCNQ**) to form ultrathin films on graphene and Au(111) surfaces is found to be due to intermolecular interactions, charge transfer from the substrate being negligible.[7,8] In other cases the strong electron attaching properties of **TCNQ** and **F_4-TCNQ** are likely responsible for doping of the substrate (or neighboring molecules) with positive holes, this effect being associated with charge transfer to the adsorbed species.[9−11] The interfacial charge transfer is known to substantially affect the electronic properties of the conjugated organic molecules in both chemisorbed and physisorbed states.[12−14] In fact, occupation of the **F_4-TCNQ** LUMO by an extra electron from the Cu(100) surface was detected using high-resolution electron energy loss spectroscopy,[15] which also indicated the presence of thermally activated morphological and orientation changes in the adsorbed species. Electron extraction from the hydrogen-terminated Si(111) surface to adsorbed **F_4-TCNQ** was also observed,[16] leading to a flat-lying anion species.

Charge transfer from the Cu(100) surface was also believed to cause thermally induced self-limited decyanation of the adsorbed **TCNQ**.[17] Electrons from the metal surface affect the **TCNQ** conformation and play a predominant role in selective decyanation.[17] P-type doping of graphene via electron transfer to the first **TCNQ** monolayer was reported to initiate surface

Received: June 12, 2014
Revised: July 28, 2014
Published: August 7, 2014

   dx.doi.org/10.1021/jp505841c | J. Phys. Chem. A 2014, 118, 6810−6818

chemical reactions with involvement of atmospheric oxygen or water, thus producing new complex organic species bearing an excess negative charge.[18] Formal cycloaddition reactions could be initialized on the Au(111) surface via consecutive deposition of porphyrin and **TCNQ** at room temperature, as reported in a scanning tunneling microscopy (STM) study,[19] the reaction being also accompanied by significant intramolecular charge transfer. Finally, it is to be mentioned that STM molecular manipulation[20] and many classes of chemical reactions on surfaces leading to generation of new molecular structures and to surface functionalization[21,22] could be initiated by low-energy electron interactions with adsorbates.[23] These reactions are likely initiated by resonance electron capture[24] followed by dissociative decay channels,[25] the process referred to as dissociative electron attachment (DEA).

DEA to isolated **TCNQ**, a molecule with a large electron-attachment cross section, could be considered as an elementary step in electron-induced surface chemistry, and its study could be useful for understanding the processes in organic semiconductors under conditions of excess negative charge. A previous gas-phase study[26] by means of electron transmission spectroscopy (ETS) determined the energies of resonance formation of temporary negative ions in **TCNQ**, whereas its DEA properties, including evaluation of the mean electron detachment time from the molecular negative ion and its slow (metastable) decomposition, have been studied using a time-of-flight apparatus.[27] The present work reports on additional dissociative channels of the temporary molecular negative ions of **TNCQ** formed by resonant electron attachment in the gas phase, thus providing data complementary to the earlier DEA study.[27] Experimental data are obtained in a different time window using a magnetic mass filter and are assigned with the support of density functional theory (DFT) calculations and the earlier ETS data.[26] The present DEA findings are discussed in connection with electron-induced chemistry and control of chemical reactions on surfaces[22] and could give some insight into the well-known problem of the low stability of organic semiconducting materials used as solar cell components.[6,28,29]

2. EXPERIMENTAL AND COMPUTATIONAL PROCEDURES

An overview of DEA spectroscopy may be found elsewhere.[25,30,31] Our apparatus coupled with a magnetic mass spectrometer has been described in detail previously[32] including a schematic representation and description of specific conditions.[33] Briefly, a magnetically collimated electron beam of defined energy was passed through the collision cell containing a vapor of the substance under investigation. The base pressure in the main vacuum chamber was about 10^{-5} Pa to ensure single-collision conditions in the collision cell (where the pressure is about 2 orders of magnitude higher). Currents of mass-selected negative ions were recorded as a function of incident electron energy in the 0−14 eV range. The electron energy scale was calibrated with the SF_6^- signal at zero energy generated by attachment of thermal electrons to SF_6. The full width at half-maximum (fwhm) of the electron energy distribution was estimated to be 0.4 eV, and the accuracy of determination of the peak position ±0.1 eV. A procedure for experimental evaluation of the electron detachment time from mass-selected negative ions modified for magnetic mass filters has been described elsewhere (see ref 34 and references therein) and is based on detection of neutral particles formed by electron detachment from the anions in the field-free region (40 cm length) before the detector. Under the present experimental conditions, the reference electron detachment time from the SF_6^- anions formed at zero electron energy was estimated to be 140 μs at 90 °C and the time-of-flight for $TCNQ^-$ from the point of its formation inside the collision cell to the detection system is estimated to be 32 μs. A suitable pressure of **TCNQ** could be achieved at 100 °C, and the walls of the collision cell were kept at 110 °C to prevent condensation. The substance under investigation is commercially available, Sigma-Aldrich product #157635, and was used without additional purification.

DFT calculations were carried out using the Gaussian09[35] program package. Evaluation of the empty orbital energies was performed using the B3LYP functional[36] and a standard 6-31G(d) basis set. Despite the difficulties encountered for an accurate description of negative ion states,[37] the occurrence of good linear correlations between the neutral-state virtual orbital energies (VOEs) and the corresponding energies of vertical electron attachment (VAEs) measured in ETS[38,39] has been demonstrated (see, for instance, refs 40−42). The scaling parameters, determined empirically, are different for σ^* and π^* states and change with the theoretical method employed.[43] Moreover, a more accurate correlation would be expected if the linear equation were calibrated with "training" compounds structurally close to the subject molecule. In the present study a scaling equation derived[44] with B3LYP/6-31G(d) calculations for π^* orbitals of alternating phenyl and ethynyl groups, VAE = (VOE + 1.14)/1.24, was employed to scale the π^* VOEs.

3. RESULTS AND DISCUSSION

Currents of mass-selected negative ions formed by DEA to gas-phase **TCNQ** as a function of incident electron energy in the 0−14 eV range are shown in Figure 1 (in order of decreasing intensity). Probable structures of the fragment negative ions, peak energies, and relative intensities are listed in Table 1 (in order of decreasing mass numbers). In agreement with previous time-of-flight experiments[27] the most intense signal in the negative-ion mass spectrum of **TCNQ** is observed at a mass-to-charge ratio (m/z) of 204, due to the formation of long-lived (microseconds) parent molecular anions $TCNQ^-$. Deflection of the charged component of the mass-selected negative-ion beam just before entrance to the detection system[34] allows detection of the neutral particles formed by electron detachment from $TCNQ^-$ anions during their flight through the field-free region (a 7 μs "time window" under present experimental conditions). The m/z = 204 signals (including the neutral component labeled $TCNQ^0$) are plotted in the 0−5 eV energy range in Figure 2 (upper panel) and compared with the SF_6^- current. The latter has an instrumental width of about 0.4 eV and peaks at zero (thermal) electron energy.

The m/z = 204 signal, associated with the formation of long-lived molecular negative ions, presents a maximum at 0.3 eV. In addition, distinct shoulders are displayed at 1.3 and 3.0 eV (Table 1). The energies of these two signals are unusually high for the observation of long-lived molecular anions. Additionally, comparison with the shape of the SF_6^- signal (Figure 2) suggests the presence of an unresolved contribution to the m/z = 204 signal also at zero energy. These findings are in very good agreement with the energies of the **TCNQ** molecular anion peaks previously observed.[27] The presence of a resonant anion state at 3 eV appears more clearly in the $TCNQ^0$ signal (upper panel of Figure 2) due to a faster electron detachment from the molecular anions, which possess a large excess energy. Its

dx.doi.org/10.1021/jp505841c | J. Phys. Chem. A 2014, 118, 6810−6818

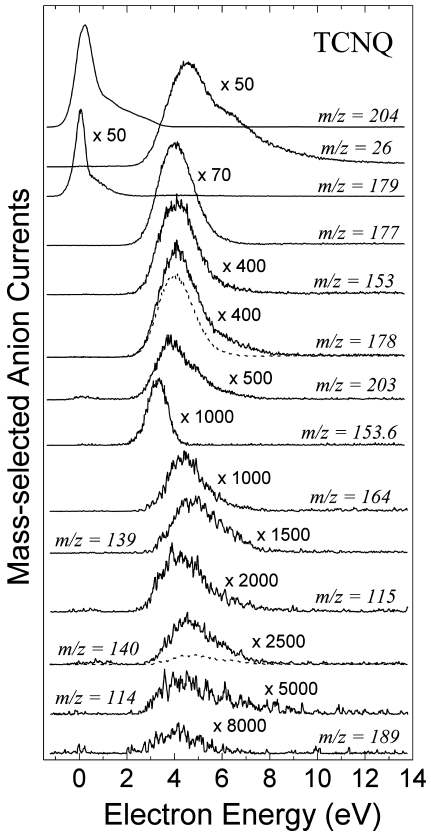

Figure 1. Current of mass-selected negative ions formed by DEA to gas-phase **TCNQ** as a function of incident electron energy. Isotopic contributions to the m/z = 178 and m/z = 140 signals are shown by dashed lines.

Table 1. Negative Ions Formed by Electron Attachment, Peak Energies (eV), and Relative Intensities Taken from Peak Maxima[a]

m/z	anion structure	peak energy	relative intensity
204	**TCNQ**$^-$	0.0 sh	
		0.3	100
		1.3 sh	
		3.0 sh	
203	[**TCNQ** − H]$^-$	3.8	0.1
		4.9 sh	
189	[**TCNQ** − NH]$^-$	4.1	<0.1
179	[**TCNQ** − C_2H]$^-$	0.0	1.7
		0.8 sh	
178	[**TCNQ** − CN]$^-$	4.0	0.1
		6.1 sh	
177	[**TCNQ** − HCN]$^-$	4.0	1.4
164	[**TCNQ** − CNN]$^-$	4.4	0.1
153.6	204 → 177	3.3	0.1
153	[**TCNQ** − CN − C_2H]$^-$	4.0	0.2
140	[**TCNQ** − $C(CN)_2$]$^-$	4.6	<0.1
139	[**TCNQ** − $CH(CN)_2$]$^-$	4.7	<0.1
115	[**TCNQ** − C_2H − $C(CN)_2$]$^-$	4.2	<0.1
114	[**TCNQ** − C_2H − $CH(CN)_2$]$^-$	4.2	<0.1
26	CN^-	4.5	2.0
		6.3 sh	

[a]sh stands for shoulder.

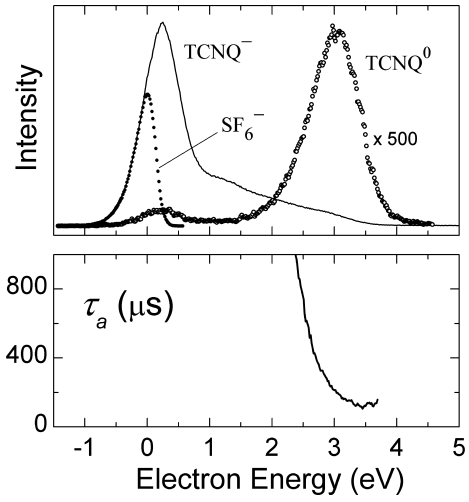

Figure 2. Upper panel: mass-selected signals of molecular negative ions and their neutral counterparts (see text). The SF_6^- signal due to thermal electron attachment to SF_6 is also reported for comparison. Lower panel: average electron detachment time from $TCNQ^-$ as a function of incident electron energy.

energy position is in agreement (within experimental limits) with the signal peaking at 3.2 eV in the time-of-flight mass spectrum.[27] Despite the low accuracy of electron detachment time measurements (see ref 34 for an overview of the sources of errors) the estimated electron detachment time (250 μs at 3 eV) from the $TCNQ^-$ negative ions formed in the 2−4 eV energy range (see lower panel of Figure 2) is in good agreement with earlier data.[27]

The only fragment anion formed by DEA to **TCNQ** below 2 eV is observed at m/z = 179 and corresponds to loss of a neutral C_2H fragment from the $TCNQ^-$ parent anion. This signal displays a maximum with a relatively high intensity (1.7% relative to the molecular anion signal at 0.3 eV) close to zero energy and a shoulder at 0.8 eV (Figure 1 and Table 1). Surprisingly, this dissociative channel (clearly observed at zero electron energy also in ref 27) was puzzling when compared to the present calculations of thermodynamic energy thresholds. The results obtained using the B3LYP/6-31+G(d) method are presented in Table 2, where the values reported in parentheses include zero-point vibrational energy (ZPE) corrections. Indeed, the most intuitive and simplest structure of the [**TCNQ** − C_2H]$^-$ fragment (labeled 3 in Chart 2) is predicted to require a thermodynamic energy threshold of 3.3 eV (Table 2), although its formation requires the minimum number of bond breaks. Rearrangement of the [**TCNQ** − C_2H]$^-$ fragment accompanied by migration of the H atoms to form four- (structure 4) and six-membered (structure 5) rings is calculated to occur only above 2 eV (Table 2). An energy threshold of 3 eV is calculated for the strongly rearranged anion fragment with structure 7, which includes a CN-substituted 1,8-naphthyridine moiety. The lowest energy threshold (1.8 eV) to form the m/z = 179 anion is calculated for the five-membered ring with structure 6 in Chart 2, but even in this case the m/e = 179 signals observed at zero energy and 0.8 eV are not accounted for by the calculations. Even accounting for about 0.3 eV of excess vibrational energy evaluated for TCNQ at 100 °C and assuming that the products can be formed in their ground vibrational states, the m/z = 179 signals observed at zero energy and 0.8 eV are not explained.

dx.doi.org/10.1021/jp505841c | J. Phys. Chem. A 2014, 118, 6810−6818

Table 2. B3LYP/6-31+G(d) Total Energies Relative to the Neutral Ground State of TCNQ[a]

m/z	fragments		relative energy (eV)
203	$[\mathbf{TCNQ} - H]^- + H^\bullet$		1.81 (1.41)
189	$[\mathbf{TCNQ} - NH]^- + NH$ (singlet)	**(1)**	6.04 (5.72)
189	$[\mathbf{TCNQ} - NH]^- + NH$ (triplet)	**(1)**	3.82 (3.49)
189	$[\mathbf{TCNQ} - NH]^- + NH$ (triplet)	**(2)**	3.81 (3.54)
179	$[\mathbf{TCNQ} - C_2H]^- + C_2H^\bullet$	**(3)**	3.76 (3.36)
179	$[\mathbf{TCNQ} - C_2H]^- + C_2H^\bullet$	**(4)**	2.84 (2.49)
179	$[\mathbf{TCNQ} - C_2H]^- + C_2H^\bullet$	**(5)**	2.44 (2.12)
179	$[\mathbf{TCNQ} - C_2H]^- + C_2H^\bullet$	**(6)**	2.15 (1.82)
179	$[\mathbf{TCNQ} - C_2H]^- + C_2H^\bullet$	**(7)**	3.32 (3.03)
178	$[\mathbf{TCNQ} - CN]^- + CN^\bullet$		1.70 (1.51)
177	$[\mathbf{TCNQ} - HCN]^-$ + HCN		1.04 (0.80)
177	$[\mathbf{TCNQ} - HCN]^- + H^\bullet + CN^\bullet$		6.79 (6.24)
164	$[\mathbf{TCNQ} - CNN]^- + {}^\bullet NCN^\bullet$	**(8)**	2.24 (1.98)
153	$[\mathbf{TCNQ} - CN - HC_2]^- + NCC_2H$	**(9)**	0.77 (0.58)
140	$[\mathbf{TCNQ} - C(CN)_2]^- + C(CN)_2$		2.74 (2.49)
139	$[\mathbf{TCNQ} - CH(CN)_2]^- + CH(CN)_2^\bullet$	**(10)**	1.68 (1.43)
115	$[\mathbf{TCNQ} - C_2H - C(CN)_2]^- + HC_3(CN)_2^\bullet$	**(11, 12)**	3.66 (3.29)
114	$[\mathbf{TCNQ} - C_2H_2 - C(CN)_2]^- + H_2C_3(CN)_2$		3.70 (3.34)
26	$CN^- + [\mathbf{TCNQ} - CN]^\bullet$		1.19 (0.99)

[a]Values in parentheses include zero-point vibrational energies. Numerical labels refer to the structures presented in Chart 2.

Although the observation of low-energy m/z = 179 signals is reproducible (and in agreement with previous DEA results[27]), the discrepancy with the calculated energy thresholds suggests possible alternative explanations for their origin. These signals could arise from the presence of trace impurities in the **TCNQ** sample. In fact, the DEA cross sections of different compounds may differ by several orders of magnitude. Another explanation could be traced back to the possible occurrence of thermal decomposition of **TCNQ** (or, its molecular negative ion) on hot metallic surfaces (filament or collision cell walls).

A series of weak decay channels of the $TCNQ^-$ molecular anion is observed above 3 eV, in agreement with previous results.[27] The most intense dissociative decay channel usually observed in compounds containing cyano groups leads to formation of the CN^- (m/z = 26) fragment anion.[30] In the present case, the CN^- negative fragment gives rise to a broad peak with a maximum at 4.5 eV (Figure 1 and Table 1), although its calculated thermodynamic energy threshold (about 1 eV, Table 2) is much lower. In contrast with previous data,[27] here CN^- is not observed at zero energy (in agreement with a calculated energy threshold of 1 eV, Table 2) nor in the 1−2 eV range. Elimination of a neutral HCN molecule from $TCNQ^-$ to form the m/z = 177 fragment anion is calculated to be energetically possible below 1 eV, but the corresponding signal is observed around 4 eV.

Due to the high sensitivity of the present experiment, various low-intensity negative fragments not reported earlier[27] were also detected. The m/z = 178 anion current cannot be entirely ascribed to the isotopic abundance of the m/z = 177 signal (Figure 1), so that some contribution may arise from formation of the $[\mathbf{TCNQ} - CN]^-$ fragment. Dehydrogenation of the $\mathbf{TCNQ}^-$ molecular negative ion, i.e., elimination of a neutral hydrogen atom from the quinone ring to form the m/z = 203 fragment, is observed at 3.8 eV, although its calculated energy threshold (about 1.5 eV, Table 2) is much smaller. A very small signal in the m/z = 203 curve observed close to zero energy is ascribed to a tail from the more intense m/z = 204 current. The m/z = 153 anion fragment, ascribed to simultaneous elimination of neutral CN and C_2H radicals from $TCNQ^-$ to form the closed-shell molecule NCC_2H (cyanoethyne) and the negative fragment with the structure labeled 9 in Chart 2, is observed around 4 eV, well above the calculated energy threshold of about 0.5 eV.

An energy threshold of 3.5 eV is calculated for the excision of neighboring hydrogen and nitrogen atoms from $TCNQ^-$ to give an NH neutral fragment in a triplet state and the geometrically rearranged m/z = 189 negative fragment with the structure labeled 1in Chart 2, in agreement with the observation of a weak m/z = 189 signal peaking at about 4

Chart 2. Likely Structures of Fragment Species Formed by DEA to TCNQ

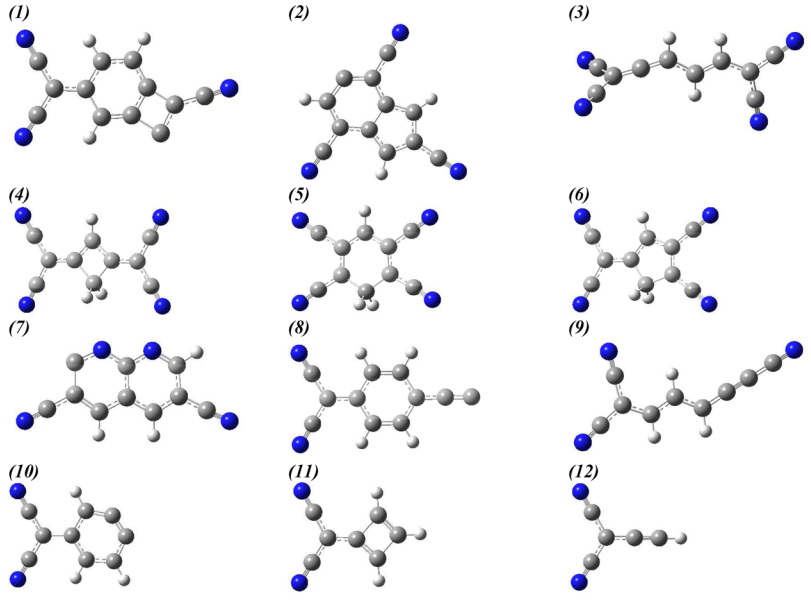

dx.doi.org/10.1021/jp505841c | J. Phys. Chem. A 2014, 118, 6810−6818

eV. A quite similar energy threshold is predicted for the negative fragment with structure 2 (Chart 2), but its formation is plausibly less probable because it would require an even stronger geometrical rearrangement. The m/z = 164 signal observed at 4.4 eV can be ascribed to elimination of an NCN neutral fragment from $TCNQ^-$ to form the anion fragment with the structure labeled 8 in Chart 1, in line with a calculated energy threshold of about 2 eV (when the NCN diradical is formed in a triplet state, the singlet state lies at about 1.4 eV higher energy). A series of less intense signals with m/z = 114, 115, 139, and 140 are observed above 4 eV and are ascribed to the loss of neutral fragments which include two CN groups, in line with the calculated energy thresholds (Tables 1 and 2, and structures labeled 10, 11, and 12 in Chart 2).

Finally, the negative ion mass spectrum of **TCNQ** recorded in the 149−158 m/z range (Figure 3) with fixed electron

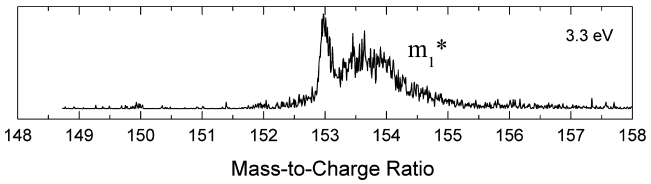

Figure 3. Negative ion mass spectrum of **TCNQ** recorded at fixed energy (3.3 eV) of the incident electron beam in the 149−158 Da mass range.

energy (3.3 eV) displays a broad and weak signal at m/z = 153.6, superimposed over the narrow m/z = 153 signal. This broad peak with fractional mass number arises from metastable (slow) dissociation of the $TCNQ^-$ molecular anion in the field-free region and corresponds to the m/z = 177 negative fragment normally formed in the acceleration region (Table 1). This metastable process was also observed using the time-of-flight technique.[27]

To assign the energies of negative ion formation measured in the ET spectrum of **TCNQ**[26] to the corresponding empty orbitals, the virtual orbital energies (VOEs) of the geometry-optimized neutral **TCNQ** molecule (Chart 3) were calculated

Chart 3. B3LYP/6-31G(d) Optimized Geometry of TCNQ

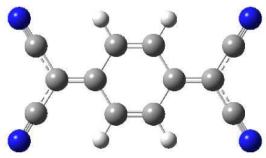

at the B3LYP/6-31G(d) level. Then the π^* VOEs were scaled with an empirically calibrated linear equation, as described in the experimental section. The scaled VOEs (SVOEs) are presented in Table 3. A schematic representation of the localization properties of the corresponding MOs is reported in Figure 4. The SVOEs nicely reproduce the measured VAEs and lead to an assignment (Table 3) of the corresponding MOs slightly different from that previously proposed.[26] The **TCNQ** neutral molecule possesses 12 empty π^* MOs, four of them (labeled π_4^*, π_5^* and π_8^*, π_9^* in Table 3 and Figure 4) are the in-plane components of the π^*_{CN} group orbitals (with σ^* local symmetry) and possess mainly CN character because they do not mix with the π^* MOs perpendicular to the molecular plane. According to the SVOEs (Table 3), electron capture into the

Table 3. B3LYP/6-31G(d) VOEs, SVOEs (See Text), and Measured VAEs Taken from Ref 26 (All Values in eV)

	B3LYP/6-31G(d)		
orbital	VOE	SVOE	VAE
			5.4
$\pi_{12}^*(b_{2g})$	4.348	4.43	4.25
$\pi_{11}^*(b_{3u})$	3.496	3.74	3.36
$\pi_{10}^*(b_{2g})$	1.385	2.04	2.12
$\pi_9^*(b_{2u})$	0.667	1.46	1.40
$\pi_8^*(b_{3g})$	0.514	1.33	
$\pi_7^*(a_u)$	0.355	1.21	1.22
$\pi_6^*(b_{1g})$	0.261	1.13	
$\pi_5^*(b_{1u})$	−0.832	0.25	0.35
$\pi_4^*(a_g)$	−0.981	0.13	
$\pi_3^*(a_u)$	−1.709	−0.46	
$\pi_2^*(b_{3u})$	−1.744	−0.49	
$\pi_1^*(b_{2g})$	−4.820	−2.97	

three lowest π^* MOs gives rise to stable anion states. The vertical EA (EA_v) predicted by the scaling procedure (2.97 eV) is close to the experimental EA values available in the literature (2.80 eV,[27] 2.88 eV[45]). The EA_v calculated with the same basis set (6-31G(d)) as the energy difference (only electronic contributions) between the neutral and anion ground states is 3.22 eV, whereas the adiabatic EA (EA_a) is found to be 3.35 eV. The relatively small difference (0.13 eV) indicates that the optimized geometry of the anion state is not too different from that of the neutral state. The use of the 6-31+G(d) basis set, which includes diffuse functions, as expected, leads to somewhat higher EA values (EA_v = 3.60 eV, EA_a = 3.73 eV). An accurate computational study of the EA of **TCNQ** by Miliàn et al.[46] pointed out that different levels of theory indicate that the EA_a of **TCNQ** should be about 0.3 eV larger than that of tetracyanoethene, experimentally determined to be 3.17 ± 0.2 eV.[47] On this basis, the EA_a of **TCNQ** would fall within the 3.2−3.7 eV range.

The π_2^* and π_3^* anion states are predicted to be stable by 0.4−0.5 eV and close in energy to each other (Table 3). The first three anion states are stable and thus not observable in ETS but are responsible for the formation (through vibrational Feshbach resonances, VFRs[25]) of the long-lived $TCNQ^-$ molecular anions observed at zero energy in the DEA spectra. The first two unstable anion states (π_4^* and π_5^*) are predicted to lie at 0.13 and 0.25 eV, respectively (Table 3). The first resonance displayed by the ET spectrum,[26] centered at 0.35 eV, could be due to the unresolved contributions of the π_4^* and π_5^* anion states. Alternatively, the signal from the former (very close to zero energy) could be masked by the high-energy side of the intense electron beam signal. The calculated SVOEs of the next two pairs of π^* MOs (π_6^*, π_7^* and π_8^*, π_9^*) lie between 1.1 and 1.5 eV, their energies closely matching the spectral features observed in the ET spectrum at 1.22 and 1.40 eV. It should be noted that the first excited (triplet) state of the neutral **TCNQ** molecule was reported to lie at about 1 eV,[26] not far from the value (0.75 eV) obtained with the present B3LYP/6-31+G(d) calculations, whereas according to previous calculations[48] the singlet−triplet excitation energy is 1.7 eV. Therefore, the shape resonances displayed by the ET spectrum above 1 eV could have contributions from core-excited states[25] of proper symmetry, these interactions being, of course, not accounted for by the calculated VOEs of the neutral ground state. The absence of negative fragments below 2 eV in the

dx.doi.org/10.1021/jp505841c | J. Phys. Chem. A 2014, 118, 6810−6818

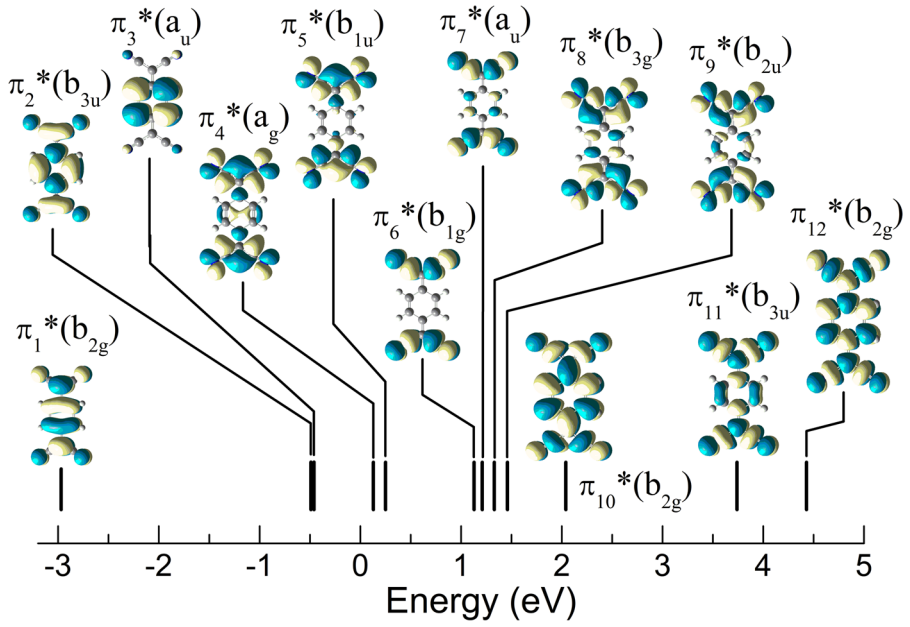

Figure 4. Localization properties and energy positions of the empty π^* orbitals of neutral **TCNQ** as predicted at the B3LYP/6-31G(d) level of theory.

DEA spectra (except for the m/z = 179 negative species discussed above) indicates that electron attachment to the $\pi_4^*-\pi_9^*$ MOs (mainly localized on the cyano groups, Figure 4) is not followed by dissociative decay of the $TCNQ^-$ parent anion. The intense ETS feature at 2.12 eV closely matches the π_{10}^* SVOE (2.04 eV, Table 3). The π_{11}^* and π_{12}^* SVOEs (3.74 and 4.43 eV) reproduce the corresponding measured VAEs (3.36 and 4.25 eV), the energy difference (0.2−0.3 eV) being in line with possible stabilization of these two resonances by mixing with higher-lying core-excited resonances. Thus, according to the present assignment the feature displayed at 5.4 eV in the ET spectrum has to be ascribed to a core-excited resonance, and not to a single particle shape resonance as previously proposed.[26] However, as mentioned earlier,[26] possible occurrence of significant configuration mixing above 4 eV is to be expected. Almost all the signals associated with dissociative decay channels of $TCNQ^-$ detected in the present work display a maximum around 4 eV (Figure 1) with a high-energy wing extending up to 6 eV. Therefore, dissociative decay of the $TCNQ^-$ molecular negative ions are essentially associated with electron attachment to the π_{12}^* MO or formation of the core-excited resonance centered at 5.4 eV.

According to the present data the π_{11}^* anion state (VAE = 3.36 eV) can follow two competing decay channels. The first consisting of the re-emission of the extra electron of the $TCNQ^-$ molecular anion, in agreement with the maximum yield of the neutral counterpart $TCNQ^0$ at 3 eV (Figure 2), with an average detachment time of 250 μs. The second decay channel of the π_{11}^* anion state consists of a slow metastable (microseconds) dissociation with elimination of an HCN neutral fragment (Table 1). The relatively narrow width of the corresponding m/z = 153.6 metastable peak (Figure 1), with a maximum at 3.3 eV, suggests that the next anion state (VAE = 4.25 eV[26]) is not involved in this slow dissociation.

In addition to formation of vibrationally excited $\pi_1^*-\pi_3^*$ anion states (VFRs), the zero-energy shoulder in the $TCNQ^-$ yield could be partly due to the π_4^* shape resonance. The observed peak energy (0.3 eV, Table 1) of the $TCNQ^-$ DEA signal matches the position (0.35 eV) of the first resonance displayed by the ET spectrum, whereas the shoulders at 1.3 and 3.0 eV correspond to the $\pi_6^*-\pi_9^*$ VAEs and the π_{11}^* VAE, respectively. Formation of long-lived $TCNQ^-$ molecular negative ions can be ascribed to the mechanism previously invoked for phthalimide[34] and anthraquinone,[49] namely, (i) initial electron capture into an unfilled MO (shape resonance) followed by (ii) rapid relaxation of this excited anion by a cascade of radiationless transitions (via accessible vacant orbitals) to its ground electronic state coupled with redistribution of the excess energy among vibrational degrees of freedom, which prevents fast electron detachment. The occurrence of the latter step is in line with the experimental observation of ultrafast (femtosecond) internal conversion of the first excited anion state of **TCNQ** into its ground state.[50]

Although formation of some fragment anionic species (m/z = 203, 178, 177, 153, 139, 26; Table 2) is calculated to be possible within the electron energy range 0.5−1.5 eV, such decays are observed in the DEA spectra around 4 eV, the only negative species present below 3 eV being the parent molecular negative ion. A plausible explanation could be traced back to a very efficient redistribution of the anion excess energy (electron affinity plus incident electron energy) among the vibrational degrees of freedom, thus preventing the possibility of concentrating into a specific vibrational mode the energy required for dissociation.

According to an inverse photoemission spectroscopy study[51] the LUMO of **TCNQ** in the solid state lies 4.2 eV below the vacuum level. The gas-phase SVOE (−3.0 eV) calculated in the present work for gas-phase **TCNQ** thus implies that the stabilization energy due to polarization forces in the solid state is about 1.2 eV, in agreement with earlier data on 3,4,9,10-perylenetetracarboxylic dianhydride and 1,4,5,8-naphthalenetetracarboxylic dianhydride (**NTCDA**).[52,53] On this basis, the π_{11}^* resonance of **TCNQ** (gas-phase VAE = 3.36 eV, Table 3) should be stabilized to about 2.2 eV in the condensed phase. In connection with electron-induced surface chemistry,[22] given that the π_{11}^* resonant state decays through metastable

dx.doi.org/10.1021/jp505841c | J. Phys. Chem. A 2014, 118, 6810−6818

dissociation of $TCNQ^-$ to produce the m/z = 177 negative fragment and an HCN neutral molecule, it could be suggested that irradiation of a **TCNQ** film with an electron beam of about 2 eV should selectively produce simultaneous decyanation and H atom abstraction via resonant formation and dissociative decay of $TCNQ^-$ negative ions. Due to the high H−C bond energy of HCN, formation of separate hydrogen and CN radicals as counterparts of the m/z = 177 anion is calculated to require more than 6 eV (Table 2). Hydrogen cyanide has been recognized as a surface active agent, for instance, causing structural changes on Pt(100).[54] Molecular transformation of HCN adsorbed on Pt(111) leads to generation of new molecular species.[55] Formation of other negative fragments (mainly CN^- observed at about 4 eV in the gas phase) would require incident electron energies above 3 eV in the solid phase. Compounds bearing a cyano group can functionalize surfaces through the formation of small organic species under the action of low-energy electrons.[56,57] Although an efficient redistribution of anion excess energy to neighboring molecules is favored in the condensed state, dissociative decay channels of temporary negative ions formed through low-energy electron interactions with adsorbed molecules often proceed via formation and decay of resonances, and mimic DEA reactions observed under gas-phase conditions.[23,58] In spite of the surface influence, dissociation of adsorbed large molecules has been found to be driven by shape resonance formation at low energies (0−4 eV) of the irradiating electron beam,[59] whereas electron stimulated desorption of the formed negative species requires higher incident electron energies.[60]

4. CONCLUSIONS

Low-energy (0−14 eV) electron attachment to the electron-acceptor **TCNQ** molecule was investigated in the gas phase by means of dissociative electron attachment (DEA) spectroscopy and the experimental findings interpreted with the support of DFT calculations of energies and localization properties of the vacant molecular orbitals and the thermodynamic thresholds for fragmentation of isolated $TCNQ^-$ molecular anions. The DEA spectra of **TCNQ** reveal unusual properties. Formation of long-lived parent molecular negative ions is detected over a wide range of incident electron energies (up to 3 eV). Moreover, slow (metastable) dissociation decay is detected at relatively high incident electron energy, where temporary molecular negative ions must store large excess energy. These findings imply that anions formed in electronically excited states can quickly convert (by a cascade of radiationless transitions) into their electronic ground state, the process being accompanied by efficient redistribution of the excess energy of excited molecular anions over a number of vibrational degrees of freedom, thus preventing fast re-emission of the extra electron. Using literature data on the electronic structure of condensed **TCNQ** and by analogy with the present gas-phase DEA results, on the one hand, we hypothesize the occurrence of surface reactions induced by irradiation with incident electrons of about 2 eV, which could stimulate simultaneous decyanation and H atom abstraction, whereas incident electron energies above 3 eV could mainly produce CN^- negative species. On the other hand, the present gas-phase DEA data show that the most abundant negative species observed below 2.5 eV by far is the parent molecular anion, the dissociative cross section being very small. Considering that in the condensed phase dissociation is further reduced by redistribution of the excess energy through collisions, the present results indicate that **TCNQ** should fulfill the requirement of long-term stability when used as an electron acceptor in solar cells or electronic devices under conditions of excess negative charge.

AUTHOR INFORMATION

Corresponding Author

*S. A. Pshenichnyuk. E-mail: sapsh@anrb.ru. Tel: +7(347)284-3538.

Notes

The authors declare no competing financial interest.

ACKNOWLEDGMENTS

S.A.P. and A.S.K. acknowledge Saint-Petersburg State University for a research grant 11.38.219.2014 and the Russian Foundation for Basic Research (grant #14-03-00087). A.M. thanks the Italian Ministero dell'Istruzione, dell'Università e della Ricerca. Thanks are due to Dr. Derek Jones (National Council of Research, Bologna, Italy) and Dr. Alexander S. Vorob'ev (Institute of Molecule and Crystal Physics, Ufa, Russia) for helpful discussion.

REFERENCES

(1) Friend, R. H.; Gymer, R. W.; Holmes, A. B.; Burroughes, J. H.; Marks, R. N.; Taliani, C.; Bradley, D. D. C.; Dos Santos, D. A.; Brédas, J. L.; Lögdlund, M.; et al. Electroluminescence in Conjugated Polymers. *Nature* **1999**, *397*, 121−128.

(2) Garnier, F.; Hajlaoui, R.; Yassar, A.; Srivastava, P. All-Polymer Field-Effect Transistor Realized by Printing Techniques. *Science* **1994**, *265*, 1684−1686.

(3) Tang, C. W. Two−Layer Organic Photovoltaic Cell. *Appl. Phys. Lett.* **1986**, *48*, 183−185.

(4) Ferraris, J.; Cowan, D. O.; Walatka, V.; Perlstein, J. H. Electron Transfer in a New Highly Conducting Donor-Acceptor Complex. *J. Am. Chem. Soc.* **1973**, *95*, 948−949.

(5) Forrest, S. R.; Thompson, M. E. Introduction: Organic Electronics and Optoelectronics. *Chem. Rev.* **2007**, *107*, 923−925.

(6) Wang, C.; Dong, H.; Hu, W.; Liu, Y.; Zhu, D. Semiconducting π-conjugated Systems in Field-Effect Transistors: A Material Odyssey of Organic Electronics. *Chem. Rev.* **2011**, *112*, 2208−2267.

(7) Barja, S.; Garnica, M.; Hinarejos, J. J.; de Parga, A. L. V.; Martín, N.; Miranda, R. Self-Organization of Electron Acceptor Molecules on Graphene. *Chem. Commun.* **2010**, *46*, 8198−8200.

(8) Torrente, I. F.; Franke, K. J.; Pascual, J. I. Structure and Electronic Configuration of Tetracyanoquinodimethane Layers on a Au (111) Surface. *Int. J. Mass Spectrom.* **2008**, *277*, 269−273.

(9) Chen, W.; Chen, S.; Qi, D. C.; Gao, X. Y.; Wee, A. T. S. Surface Transfer p-Type Doping of Epitaxial Graphene. *J. Am. Chem. Soc.* **2007**, *129*, 10418−10422.

(10) Qi, D.; Chen, W.; Gao, X.; Wang, L.; Chen, S.; Loh, K. P.; Wee, A. T. Surface Transfer Doping of Diamond (100) by Tetrafluorotetracyanoquinodimethane. *J. Am. Chem. Soc.* **2007**, *129*, 8084−8085.

(11) Gao, W.; Kahn, A. Controlled p-Doping of Zinc Phthalocyanine by Coevaporation with Tetrafluorotetracyanoquinodimethane: A Direct and Inverse Photoemission Study. *Appl. Phys. Lett.* **2001**, *79*, 4040−4042.

(12) Godlewski, S.; Szymonski, M. Adsorption and Self-Assembly of Large Polycyclic Molecules on the Surfaces of TiO2 Single Crystals. *Int. J. Mol. Sci.* **2013**, *14*, 2946−2966.

(13) Grządziel, L.; Krzywiecki, M.; Peisert, H.; Chassé, T.; Szuber, J. Photoemission Study of the Si(111)-Native SiO2/Copper Phthalocyanine (CuPc) Ultra-Thin Film Interface. *Org. Electron.* **2012**, *13*, 1873−1880.

(14) Komolov, A. S.; Møller, P. J. Photoconductivity and Oxygen Adsorption on Cu-Phthalocyanine Films on Cadmium Sulphide. *Appl. Surf. Sci.* **2003**, *212−215*, 497−500.

(15) Katayama, T.; Mukai, K.; Yoshimoto, S.; Yoshinobu, J. Thermally Activated Transformation from a Charge-Transfer State to a Rehybridized State of Tetrafluoro-tetracyanoquinodimethane on Cu (100). *J. Phys. Chem. Lett.* **2010**, *1*, 2917−2921.
(16) Furuhashi, M.; Yoshinobu, J. Charge Transfer and Molecular Orientation of Tetrafluoro-tetracyanoquinodimethane on a Hydrogen-Terminated Si (111) Surface Prepared by a Wet Chemical Method. *J. Phys. Chem. Lett.* **2010**, *1*, 1655−1659.
(17) Urban, C.; Wang, Y.; Rodríguez-Fernández, J.; García, R.; Herranz, M. Á.; Alcamí, M.; Martín, N.; Martín, F.; Gallego, J. M.; Miranda, R.; Otero, R. Charge Transfer-Assisted Self-Limited Decyanation Reaction of TCNQ-type Electron Acceptors on Cu (100). *Chem. Commun.* **2014**, *50*, 833−835.
(18) Qi, Y.; Mazur, U.; Hipps, K. W. Charge Transfer Induced Chemical Reaction of Tetracyano-p-quinodimethane Adsorbed on Graphene. *RSC Adv.* **2012**, *2*, 10579−10584.
(19) Fesser, P.; Iacovita, C.; Wäckerlin, C.; Vijayaraghavan, S.; Ballav, N.; Howes, K.; Gisselbrecht, J.-P.; Crobu, M.; Boudon, C.; Stöhr, M.; et al. Visualizing the Product of a Formal Cycloaddition of 7,7,8,8-Tetracyano-p-quinodimethane (TCNQ) to an Acetylene-Appended Porphyrin by Scanning Tunneling Microscopy on Au (111). *Chem.-A Eur. J.* **2011**, *17*, 5246−5250.
(20) Mayne, A. J., Dujardin, G., Eds. *Atomic and Molecular Manipulation*; Elsevier: Amsterdam, 2011.
(21) Sakulsermsuk, S.; Sloan, P. A.; Palmer, R. E. A New Mechanism of Atomic Manipulation: Bond-Selective Molecular Dissociation via Thermally Activated Electron Attachment. *ACS Nano* **2010**, *4*, 7344−7348.
(22) Böhler, E.; Warneke, J.; Swiderek, P. Control of Chemical Reactions and Synthesis by Low-Energy Electrons. *Chem. Soc. Rev.* **2013**, *42*, 9219−9231.
(23) Arumainayagam, C. R.; Lee, H. L.; Nelson, R. B.; Haines, D. R.; Gunawardane, R. P. Low-Energy Electron-Induced Reactions in Condensed Matter. *Surf. Sci. Rep.* **2010**, *65*, 1−44.
(24) Palmer, R. E.; Rous, P. J. Resonances in Electron Scattering by Molecules on Surfaces. *Rev. Mod. Phys.* **1992**, *64*, 383−440.
(25) Schulz, G. J. Resonances in Electron Impact on Atoms. Resonances in Electron Impact on Diatomic Molecules. *Rev. Mod. Phys.* **1973**, *45* (378−422), 423−486.
(26) Burrow, P. D.; Howard, A. E.; Johnson, A. R.; Jordan, K. D. Temporary Anion States of Hydrogen Cyanide, Methyl Cyanide, and Methylene Dicyanide, Selected Cyanoethylenes, Benzonitrile, and Tetracyanoquinodimethane. *J. Phys. Chem.* **1992**, *96*, 7570−7578.
(27) Compton, R. N.; Cooper, C. D. Negative Ion Properties of Tetracyanoquinodimethan: Electron Affinity and Compound States. *J. Chem. Phys.* **1977**, *66*, 4325−4329.
(28) Modelli, A.; Jones, D.; Pshenichnyuk, S. A. Electron Attachment to Dye-Sensitized Solar Cell Components: Rhodanine and Rhodanine-3-acetic Acid. *J. Phys. Chem. C* **2009**, *114*, 1725−1732.
(29) Modelli, A.; Burrow, P. D. Electron Attachment to Dye-Sensitized Solar Cell Components: Cyanoacetic Acid. *J. Phys. Chem. A* **2011**, *115*, 1100−1107.
(30) Illenberger, E.; Momigny, J. *Gaseous Molecular Ions. An Introduction to Elementary Processes Induced by Ionization*; Steinkopff Verlag Darmstadt, Springer-Verlag: New York, 1992.
(31) Christophorou, L. G. *Electron-Molecule Interactions and their Applications*; Academic Press: Orlando, 1984.
(32) Khvostenko, V. I. *Negative Ions Mass Spectrometry in Organic Chemistry*; Nauka: Moscow, 1981 (in Russian).
(33) Pshenichnyuk, S. A.; Asfandiarov, N. L. The Role of Free Electrons in MALDI: Electron Capture by Molecules of α-Cyano-4-hydroxycinnamic Acid. *Eur. J. Mass Spectrom.* **2004**, *10*, 477−486.
(34) Pshenichnyuk, S. A.; Vorob'ev, A. S.; Modelli, A. Resonance Electron Attachment and Long-lived Negative Ions of Phthalimide and Pyromellitic Diimide. *J. Chem. Phys.* **2011**, *135*, 184301/1−11.
(35) Frisch, M. J.; Trucks, G. W.; Schlegel, H. B.; Scuseria, G. E.; Robb, M. A.; Cheeseman, J. R.; Scalmani, G.; Barone, V.; Mennucci, B.; Petersson, G. A.; et al. *Gaussian 09*, Revision A.02; Gaussian, Inc., Wallingford, CT, 2009.
(36) Becke, A. D. Density-functional Thermochemistry. III. The Role of Exact Exchange. *J. Chem. Phys.* **1993**, *98*, 5648−5652.
(37) Simons, J.; Jordan, K. D. Ab Initio Electronic Structure of Anions. *Chem. Rev.* **1987**, *87*, 535−555.
(38) Jordan, K. D.; Burrow, P. D. Temporary Anion States of Polyatomic Hydrocarbons. *Chem. Rev.* **1987**, *87*, 557−588.
(39) Modelli, A. Gas-phase Empty Level Structure in Heterosubstituted Hydrocarbons and Organometallic Compounds by Means of Electron Transmission Spectroscopy. *Trends Chem. Phys.* **1997**, *6*, 57−95.
(40) Chen, D. A.; Gallup, G. A. The Relationship of the Virtual Orbitals of Self-consistent-field Theory to Temporary Negative Ions in Electron Scattering from Molecules. *J. Chem. Phys.* **1990**, *93*, 8893−8901.
(41) Staley, S. W.; Strnad, J. T. Calculation of the Energies of pi* Negative Ion Resonance States by the Use of Koopmans' Theorem. *J. Phys. Chem.* **1994**, *98*, 116−121.
(42) Modelli, A. Electron Attachment and Intramolecular Electron Transfer in Unsaturated Chloroderivatives. *Phys. Chem. Chem. Phys.* **2003**, *5*, 2923−2930.
(43) Burrow, P. D.; Modelli, A. On the Treatment of LUMO Energies for Their Use as Descriptors. *SAR QSAR Environ. Res.* **2013**, *24*, 647−659.
(44) Scheer, A. M.; Burrow, P. D. π* Orbital System of Alternating Phenyl and Ethynyl Groups: Measurements and Calculations. *J. Phys. Chem. B* **2006**, *110*, 17751−17756.
(45) Farragher, A. L.; Page, F. M. Experimental Determination of Electron Affinities. Part II. - Electron Capture by Some Cyanocarbons and Related Compounds. *Trans. Faraday Soc.* **1967**, *63*, 2369−2378.
(46) Milián, B.; Pou-AméRigo, R.; Viruela, R.; Ortí, E. On the Electron Affinity of TCNQ. *Chem. Phys. Lett.* **2004**, *391*, 148−151.
(47) Chowdhury, S.; Kebarle, P. Electron Affinities of Di- and Tetracyanoethylene and Cyanobenzenes Based on Measurements of Gas-phase Electron-Transfer Equilibria. *J. Am. Chem. Soc.* **1986**, *108*, 5453−5459.
(48) Herman, F.; Batra, I. P. Electronic Structure of the Tetracyanoquinodimethane (TCNQ) Molecule. *Phys. Rev. Lett.* **1974**, *33*, 94−97.
(49) Pshenichnyuk, S. A.; Vorob'ev, A. S.; Asfandiarov, N. L.; Modelli, A. Molecular Anion Formation in 9,10-anthraquinone: Dependence of the Electron Detachment Rate on Temperature and Incident Electron Energy. *J. Chem. Phys.* **2010**, *132*, 244313/1−10.
(50) Roberts, G. M.; Lecointre, J.; Horke, D. A.; Verlet, J. R. Spectroscopy and Dynamics of the 7,7,8,8-Tetracyanoquinodimethane Radical Anion. *Phys. Chem. Chem. Phys.* **2010**, *12*, 6226−6232.
(51) Kanai, K.; Akaike, K.; Koyasu, K.; Sakai, K.; Nishi, T.; Kamizuru, Y.; Nishi, T.; Ouchi, Y.; Seki, K. Determination of Electron Affinity of Electron Accepting Molecules. *Appl. Phys. A: Mater. Sci. Process.* **2009**, *95*, 309−313.
(52) Pshenichnyuk, S. A.; Komolov, A. S. Relation between Electron Scattering Resonances of Isolated NTCDA Molecules and Maxima in the Density of Unoccupied States of Condensed NTCDA Layers. *J. Phys. Chem. A* **2012**, *116*, 761−766.
(53) Pshenichnyuk, S. A.; Kukhto, A. V.; Kukhto, I. N.; Komolov, A. S. Spectroscopic States of PTCDA Negative Ions and Their Relation to the Maxima of Unoccupied State Density in the Conduction Band. *Technol. Phys.* **2011**, *56*, 754−759.
(54) Bridge, M. E.; Lambert, R. M. Adsorption, Reactivity and Surface Structural Chemistry of Hydrogen Cyanide on Pt (110). *J. Catalys.* **1977**, *46*, 143−150.
(55) Jentz, D.; Celio, H.; Mills, P.; Trenary, M. Formation of Aminomethylidyne from Hydrogen Cyanide on Pt (111). *Surf. Sci.* **1995**, *341*, 1−8.
(56) Lafosse, A.; Bertin, M.; Caceres, D.; Jäggle, C.; Swiderek, P.; Pliszka, D.; Azria, R. Electron Induced Functionalization of Diamond by Small Organic Groups. *Eur. Phys. J. D* **2005**, *35*, 363−366.
(57) Ipolyi, I.; Michaelis, W.; Swiderek, P. Electron-Induced Reactions in Condensed Films of Acetonitrile and Ethane. *Phys. Chem. Chem. Phys.* **2007**, *9*, 180−191.

(58) Mason, N. J. Electron-Induced Chemistry: A Forward Look. *Int. J. Mass Spectrom.* **2008**, *277*, 31−34.
(59) Martin, F.; Burrow, P. D.; Cai, Z.; Cloutier, P.; Hunting, D.; Sanche, L. DNA Strand Breaks Induced by 0−4 eV Electrons: The Role of Shape Resonances. *Phys. Rev. Lett.* **2004**, *93*, 068101/1−4.
(60) Tegeder, P.; Illenberger, E. Electron Stimulated Desorption of Anions from Condensed XCN (X= Cl, Br): State Selectivity in the Desorption Spectra of Fragment Anions. *Chem. Phys. Lett.* **2005**, *411*, 175−180.